

Supporting Information

Determination of Quantum Capacitance and Band Filling Potential in Graphene Transistors with Dual Electrochemical and Field-Effect Gates

*Chang-Hyun Kim, C. Daniel Frisbie**

Department of Chemical Engineering and Materials Science, University of Minnesota, 421
Washington Avenue SE, Minneapolis, Minnesota 55455, United States

*Corresponding Author. Phone: 612-625-0779 / E-mail: frisbie@umn.edu

S1. Raman Analysis of CVD Graphene Transferred on Si⁺⁺/SiO₂ Wafer

We performed the Raman analysis to identify the phases of the CVD graphene used in this study. The areas with higher contrast in the optical image in Figure S1b, which are believed to be multilayer graphene phases, have either the *multilayer* spectrum or the *monolayer* spectrum with a stronger signal. The phases of the latter case are likely composed of loosely coupled monolayers with a different stacking order.¹ The Raman spectrum at each point could be deconvoluted into a linear combination of the average spectra of *monolayer* and *multilayer* spectra shown in Figure S1a, and no significant D peak ($\sim 1360\text{ cm}^{-1}$) was observed on our sample. The CVD graphene consists of $\sim 82\%$ monolayer phase and $\sim 18\%$ multilayer islands with $\sim 1\text{-}3\text{ }\mu\text{m}$ sizes.

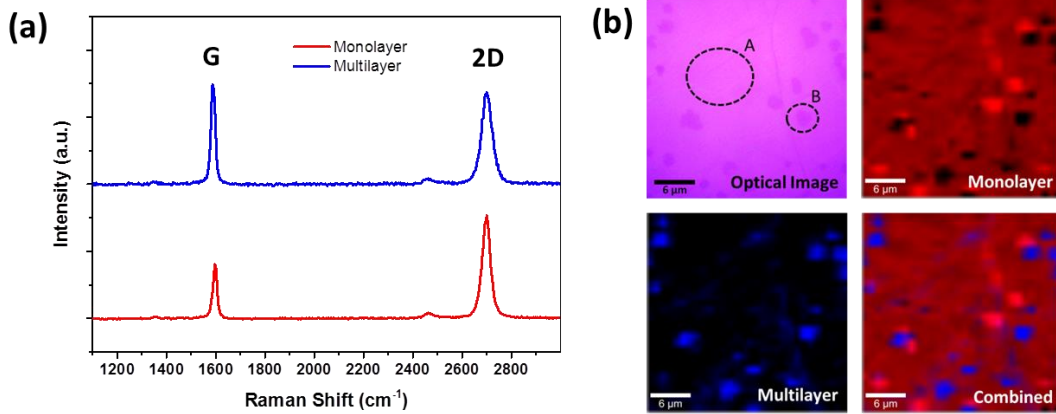


Figure S1. (a) The average Raman spectra of monolayer and multilayer graphene phases, which were obtained from the internal standard points (A and B indicated in optical image of (b)). (b) The optical image and the corresponding spectral Raman map of CVD graphene transferred on Si⁺⁺/SiO₂ wafer. The red and blue spots indicate monolayer and multilayer phases, respectively.

S2. Hysteresis in Transfer Curves of Back- and Electrolyte-Gated G-FETs.

Figure S2 shows the transfer curves of G-FETs in forward and reverse sweep of (a-c) back-gating and (d) electrolyte-gating modes, respectively. While negligible hysteresis was observed in I_{SD} - V_{BG} curve before ion gel printing (Figure S2a), significant hysteresis was observed at the same V_{BG} sweep rate after ion gel printing (Figure S2b). Recently, Levesque et al.² demonstrated that the charge transfer between graphene and adjacent donors/acceptors (*e.g.* O_2/H_2O molecules adsorbed on the graphene surface) is an important mechanism that causes large hysteresis in I_{SD} - V_{BG} curves. Likewise, when the Fermi-level in the graphene channel shifts to a sufficiently high energy level at $V_{BG} \gg 0$ V in our device, the electrons induced in the graphene channel can transfer to adjacent electron acceptors in ion gel phase rather than reside in the graphene channel. Because this charge transfer reduces the number of electrons in graphene channel at $V_{BG} \gg 0$ V, the Dirac point is observed at more positive V_{BG} in the reverse sweep (Figure S2b). The hysteresis leads to less accurate estimation of charge carrier density and quantum capacitance C_Q (especially at high V_{BG}), and thus should be minimized. In this work, smaller hysteresis could be

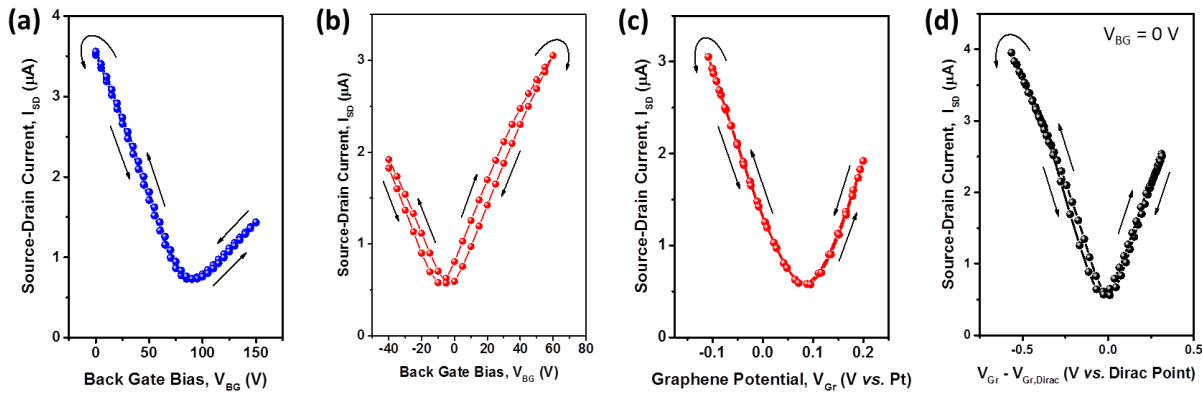


Figure S2. Source-to-drain current vs. back-gate bias (I_{SD} - V_{BG}) curves of the G-FET (a) before ion gel printing and (b) after ion gel printing obtained at $V_{SD}=10$ mV and $dV_{BG}/dt = \pm 29.5$ V/s. (c) Source-to-drain current vs. graphene potential (I_{SD} - V_{Gr}) curve of the ion gel printed G-FET, in which V_{Gr} was simultaneously measured during the back-gating mode (b). (d) I_{SD} - V_{Gr} curve obtained at $V_{SD}=10$ mV and $dV_{EG}/dt = \pm 0.59$ V/s. Note that only forward sweep curves are presented and used for data analysis in the main manuscript.

achieved by increasing the V_{BG} sweep rate because under this condition the Fermi-level stays at high energy states for shorter time, which minimizes charge transfer between graphene and the electrolyte.

Negligible hysteresis is observed in the I_{SD} - V_{Gr} curve (Figure S2c), where V_{Gr} was simultaneously measured in the back-gating mode (Figure S2b). This shows that V_{Gr} , rather than V_{BG} , is a good indicator of charge carrier density in the graphene channel especially when there is significant charge transfer between graphene and ion gel phase.

Lastly, we observed little but observable hysteresis in I_{SD} - V_{Gr} curves in the electrolyte-gating mode (Figure S2d). It is believed that this small hysteresis comes from relatively slow ionic transport, which does not occur in back-gating mode, compared to carrier injection into the graphene channel—the slow ion transport prohibits the EDL structure at the graphene/ion gel interface from reaching thermodynamic equilibrium and thus V_{Gr} at a given carrier density in graphene can have different values in the forward and reverse sweeps.

S3. Carrier Transport in Dual-Gated G-FETs.

From the obtained C_Q and C_{EDL} data, the V_{Gr} shifts required in back-gating ($-\delta$) and in electrolyte-gating ($-\delta - \Delta\phi_{EDL}$) at a fixed back-gate bias can be expressed as a function of n_{ind} using the following equation.

$$n_{ind} = -\frac{1}{e} \int_0^\delta C_Q d\delta = -C_{EDL}(\phi_{EDL} - \phi_{EDL,Dirac})/e \quad (S1)$$

Using the V_{Gr} - n_{ind} relationships (Figure S3), the data in Figure 6a are converted to R_S - n_{ind} curves and fit to the model of equations 1 and 2 (shown in Figure S4). The curves are well fit to the model for the overall V_{BG} range, which suggests that the electrochemical potential at a given dual-gating condition can also be reproduced by adding band-filling potential ($-\delta$) and double-layer charging potential ($-\Delta\phi_{EDL}$) to the electrochemical potential at the Dirac point shown in Figure 6b.

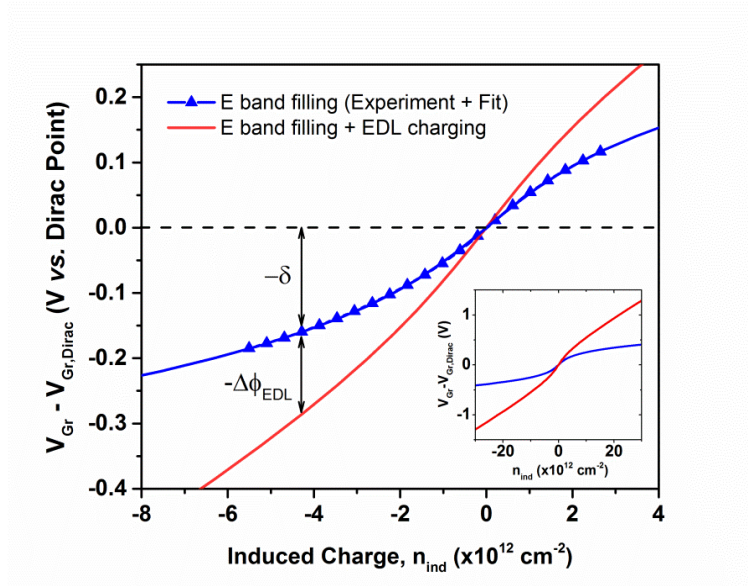


Figure S3. Electrochemical potential shift required in back-gating (blue triangles and solid line represent experimental data and curve fitting result in which the quantum capacitance of graphene (C_Q) in Figure 3b is approximated as a second order polynomial of δ , respectively) and in electrolyte-gating (red solid line, calculated) as a function of induced charge density in graphene channel. Inset shows the curves in a larger scale. Note that the electrochemical potential shift in electrolyte gating ($-\delta - \Delta\phi_{EDL}$) is calculated from equation S1.

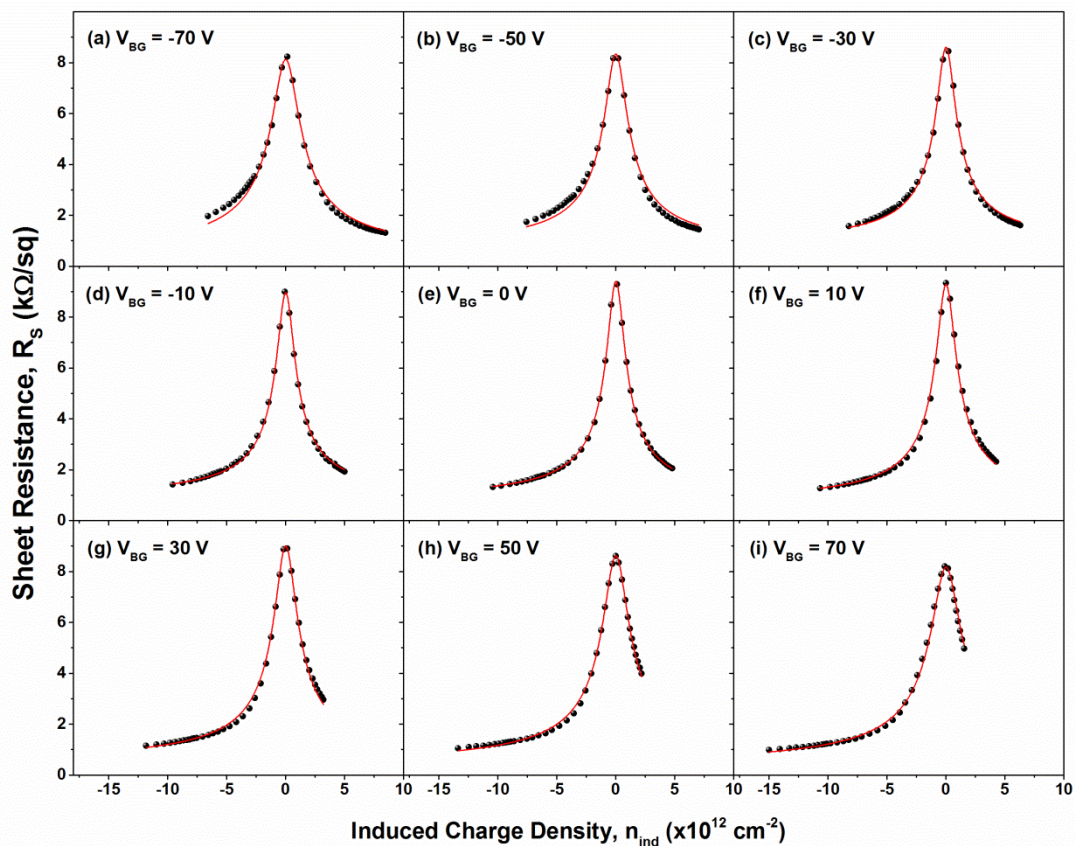


Figure S4. Black circles in (a)-(i) represent the sheet resistance as a function of electrolyte-gate induced charge density in graphene channel which were obtained at fixed V_{BG} from -70 to 70 V. Red lines represent the curves fit to the Drude model of equations 1 and 2.

REFERENCE

- (1) Kim, K.; Coh, S.; Tan, L. Z.; Regan, W.; Yuk, J. M.; Chatterjee, E.; Crommie, M. F.; Cohen, M. L.; Louie, S. G.; Zettl, a. Raman Spectroscopy Study of Rotated Double-Layer Graphene: Misorientation-Angle Dependence of Electronic Structure. *Phys. Rev. Lett.* **2012**, *108*, 246103.
- (2) Levesque, P. L.; Sabri, S. S.; Aguirre, C. M.; Guillemette, J.; Siaj, M.; Desjardins, P.; Szkopek, T.; Martel, R. Probing Charge Transfer at Surfaces Using Graphene Transistors. *Nano Lett.* **2011**, *11*, 132–137.